TRANSITION TO TURBULENCE AND RELAMINARIZATION PHENOMENA IN THE FLOW BETWEEN TWO ROTATING SPHERES

M. Mahloul[1], A. Mahamdia[1] and V. Sobolik[2]

[1]Faculty of Physics, University of Sciences and Technology Houari Boumediene, BP N° 32 El Alia 16111 Algiers – Algeria

[2]LaSIE, University of La Rochelle, Avenue Michel Crépeau, 17042 La Rochelle, France

Abstract

Modes selection of different instabilities that lead to turbulence between two concentric spheres, the inner rotating while the outer is at rest, is investigated through visualization and polarography method. The exploration of the flow regimes was carried out for a dimensionless gap width $\delta = (R_2-R_1)/R_1$ of 0.107, an aspect ratio $\Gamma=H/d$ in the interval (17; 21) and a Taylor number in the interval (22; 1500). The influence of these parameters on the appearance of instabilities is elucidated. The evolution of the flow patterns is visualized and quantified by the wall velocity gradients and their fluctuations. The case considered here is closely related to the polarographic method in a spherical shell. At our best knowledge, this has not been studied to the present day.

Keywords: Spherical Taylor-Couette, concentric spheres, vortex, instability, polarography

1 Introduction

The spherical Taylor-Couette flow is an important research topic since many years. Its scientific relevance lies not only in the simplicity of the system but also in its applicability to astrophysical objects and geophysical motions such as atmospheres, oceans, and planetary cores.

The first instability of the basic flow leads to the formation of Taylor vortices in the equatorial region, as reported by Khlebutin [1], Sawatzki [2], Munson [3], Yavorskaya [4], Wimmer [5,6], Bühler [7,8], Schrauf, G. [9], C. Egbers [10] and R. Hollerbach [11].

Khlebutin [1] was the first who experimentally detected the existence of Taylor cells in a spherical flow system for a dimensionless gap range of $0.19 \leq \delta \leq 0{,}371$. He carried out flow visualization experiments and torque measurements in the range of $0.037 \leq \delta \leq 1.515$, but for $\delta \geq 0.44$, no Taylor vortices were observed. C. Egbers and H.J. Rath [10] have investigated experimentally of the existence of Taylor vortices and different instabilities in spherical Couette flow. For wide gaps ($0.33 \leq \delta \leq 0.5$), however, Taylor vortices could not be detected. Wimmer [12] showed that the flow modes could be produced by different acceleration histories of the inner sphere.

Another study on torque measurements as a function of flow regimes was done by Munson and Menguturk [3]. Koichi Nakabayachi et al [13] traced the evolution of non-dimensional RMS (root mean square) values of V_φ and V_θ divided by U_0. V_φ and V_θ stand for fluctuations of azimuthal and meridian velocity components, respectively. U_0 stands for peripheral velocity of rotating inner sphere. D. Schmitt et al [14] have studied experimentally a rotating spherical Couette flow in a dipolar magnetic field. They focus on the time dependence of the electric potential differences between electrodes located on the outer sphere and on the time correlations between these differences. On the other hand, several numerical studies were carried out. Bar-Yoseph et al. [15,16] treated both

concentric and eccentric spherical gaps for two different radii ratios of a medium size gap by means of finite-element method. Mamun and Tuckerman [17] examined asymmetry and Hopf bifurcation in spherical Couette flow using Newtonian fluids. They presented bifurcation diagrams along with torque characteristics. R J Yang [18] applied in his simulations of the axisymmetric flow fictitious symmetric boundary conditions to find all possible flow modes. Li Yuan [19] has discussed the wavy and spiral Taylor-Gortler vortices in medium spherical gaps (δ=0.14 and 0.18). Kelly et al. [20] studied linear wave modes restored by the Coriolis force. They proposed selection mechanisms to explain the presence of the particular observed modes.

We aim, in this paper at exploring experimentally the spherical Taylor-Couette flow. The ultimate goal is the evolution of the structures during the laminar-turbulent transition. The results obtained allow us to present the evolutions of the velocity gradient S and the fluctuating rate s'/S as a function of the Taylor number for different values of the aspect ratio Γ.

2 Experimental conditions

The experimental setup consists of two concentric spheres made of transparent Plexiglas, with the inner sphere rotating and the outer one stationary (Fig.1). The outer and inner spheres have a radius of R_2=54.9 mm and R_1= 49.6mm, respectively. The corresponding non-dimensional gap width $\delta = d/R_1$ is equal to 0.107. The definitions of geometrical parameters are similar to that used in cylindrical Taylor-Couette systems, i.e. the gap width $d = R_2 - R_1 = 5.3$ mm and the aspect ratio $\Gamma = H / d$ where H is the height of liquid varying in the spherical gap. Another important control-parameter coming into account is the acceleration rate. This because the occurring flow pattern during the transition to turbulence are also determined by the history of the flow, i.e. it depends on whether the Taylor number is increased or decreased, quasi stationary or fast.

The inner sphere is driven by a dc motor at a speed between 0.01 and 3.01rev/s. The fluid temperature is given by a digital thermometer and maintained constant within 0.1°C. The working fluid is an aqueous solution of ferri-ferro-potassium cyanide in an equimolar concentration of 2 mol/m^3 with an excess chloride of potassium (300kg/m^3). Four platinum probes 0.5 mm diameter served as cathodes and were flush mounted with the inner wall of the outer sphere at angles of θ_1= 82.5°, θ_2= 84°, θ_3= 85.5° and θ_4= 88.5° (Fig. 1). The anode was a platinum sheet (50×20mm) fixed at the bottom of the outer sphere.

The electrochemical method has been applied to the study of Taylor-Couette systems since the early 1970s by Cognet [21]. This method makes use of the mass transfer in the vicinity of the working (measuring) electrode. The principle of this method is to impose on the measuring electrode (probe) a potential which is different from the equilibrium one. In this way an electrochemical reaction takes place and the probe active surface in contact with the solution becomes the site of ion exchange. The motion of ions is the result of the migration motion due to the electrical field, of the convection of the flow circulation and of the molecular diffusion due to the gradient concentration of active ions in the bulk of the liquid and on the electrode. The migration is suppressed by addition of a supporting electrolyte (potassium chloride). In the quasi-steady boundary layer approximation (Leveque, [22]) the velocity gradient S at the electrode is related to the limiting diffusion current by the relation

$$S = 0.0996 \frac{I^3}{(nFc)^3 D^2 R^5} \tag{1}$$

where I is the measured electric current, D the diffusion coefficient, R the electrode radius, F the Faraday constant, n the number of electrons involved in the electrochemical reaction and c the concentration of active species in the bulk.

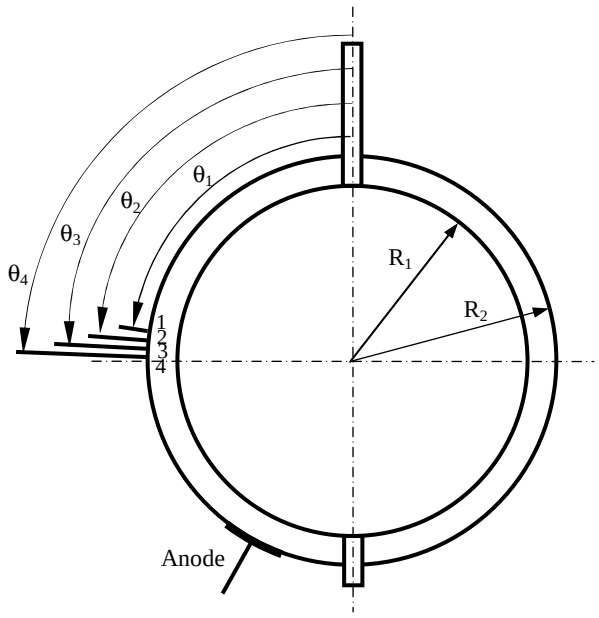

Figure 1: Experimental setup. 1, 2, 3, 4 stand for measuring electrodes.

The flow structures were visualized by adding 2% by volume of Kalliroscope into the electrochemical solution. Video and limiting diffusion currents were recorded simultaneously. The analysis of the measured current permitted the study of temporal variations of flows. The signals were treated in two stages: firstly the mean component was calculated by averaging the signal recorded during 5 min, and then the signal is high pass filtered to remove the mean component and to obtain only the fluctuations intensity. The analogical-digital conversion is by means of a PC-card (NI 6008) connected to a computer. The temporal behavior of the flow was characterized by power spectra that were obtained by FFT MATLAB algorithm.

3 Results

Different flow stages were identified in terms of the Taylor number, defined as:

$$Ta = \frac{R_1 \Omega d}{\nu} \sqrt{\frac{d}{R_1}} \tag{2}$$

where Ω is the angular velocity of the inner sphere and ν the kinematic viscosity. The following paragraphs describe the flow patterns and wall velocity gradient corresponding to particular ranges of the Taylor number which were adjusted by variation of angular velocity.

Flow without Taylor vortices, Ta<44

The rotation rate of the inner sphere was quasi statically increased from rest. For Taylor numbers in the interval 0<Ta<44, the flow is stable and no structures are observed. As Ta close to 0, the flow is characterized by streamlines in the form of concentric circles with circumferential velocity component expressed by (Bühler [8])

$$v(r,\vartheta)=\frac{\Omega R_1^3(r^3-R_2^3)}{r^2(R_1^3-R_2^3)}\sin\theta \qquad (3)$$

There is a balance between inertial forces and viscous forces. The meridian and radial velocity components are zero. As Ta close to 0 the wall velocity gradient at the outer sphere yield:

$$S=-\left.\frac{\partial v}{\partial r}\right|_{r=R_2}=\frac{3\Omega R_1^3}{R_2^3-R_1^3}\sin\theta \qquad (4)$$

For higher values of Ta, the meridian and radial velocity components are non zero and the streamlines form spirals oriented from equator to the pole at the outer sphere and in the inverse direction at the inner sphere (Bühler [8]). However, this secondary flow is so slow that the spirals are not visible. The measured wall velocity gradient corresponds practically to Eq. (4). Bartels [23] and Bühler [8] denote this flow as mode I. In the laminar flow Ta<44 the measured velocity gradient is proportional to Taylor number S~Ta.

Taylor vortices, 44 < Ta < 47

At the critical value of Taylor number Tc_1 = 44, the onset of Taylor vortices took place. The final flow structure is composed of four cells, i.e. a symmetrical configuration of a pair of cells on each side of the equator (Fig.2). The streamlines in the rest of spherical gap still have a form of spirals. They are not visible due to slow motion. However, the onset of the first instability for SCF was approximately given by $Re_c = 49\delta^{-3/2}$, Khlebutin [1]; after that, this power law was improved to $Re_c = 41.3(1+\delta)^{-3/2}$ for $\delta<0.3$ (Nakabayashi [24]).

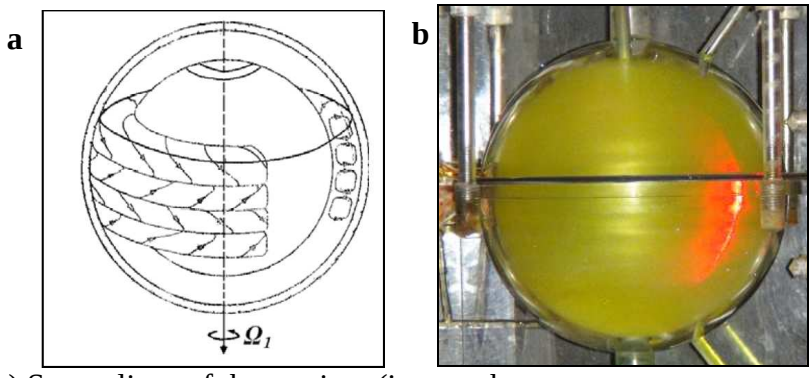

Figure 2: (a) Streamlines of the vortices (inner sphere rotates, outer one at rest, Wimmer [12]), (b) Visualization of the first instability at Tc_1= 44,Γ=20.75.

On the other hand, the wall velocity gradients measured by three probes are shown in Fig. 3.They increase slightly in this range.

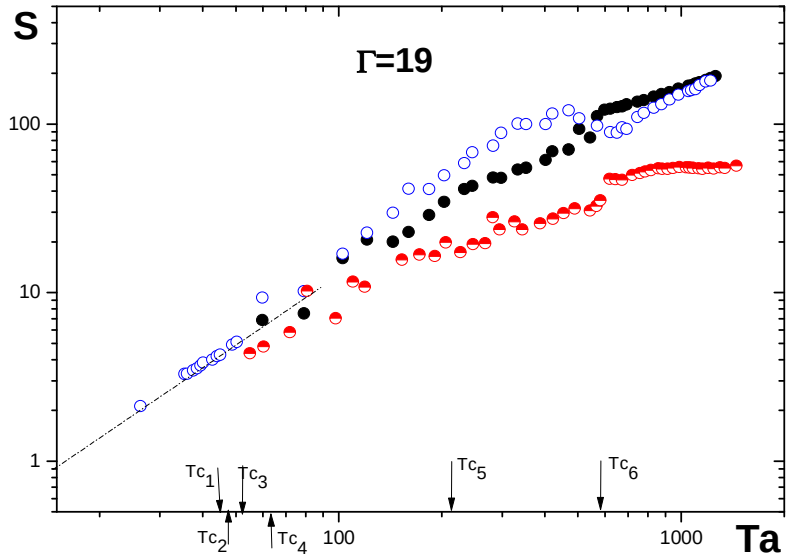

Figure 3: Evolution of the mean wall velocity gradient versus Taylor number. Open circles stand for probe 1and solid circles for probe 3.

Taylor vortices and spirals, 47 ≤Ta < 53

At the Taylor number Tc_2= 47, a second regime occurred. The flow took a form of four Taylor cells at the equator and four spirals at each hemisphere; see sketch in Fig. 4a. The spirals are inclined between 2° and 10° with respect to the equator. As the angular velocity was further increased, additional spirals appeared and occupy the entire fluid. An increase in wall velocity gradient was observed at the two probes (Fig.3), but the values were still independent of time indicating that the flow was stationary.

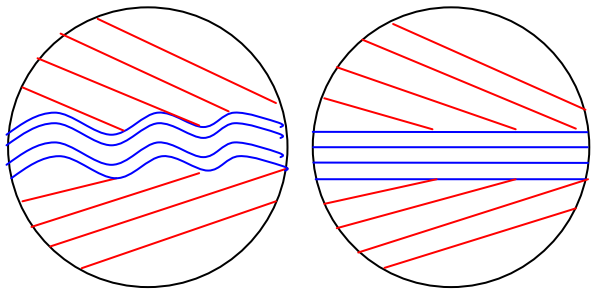

Figure 4: (a) Taylor cells and spirals. (b) Wavy Taylor cells and spirals.

The non-dimensional fluctuations intensity, s'/S, values sharply increase with the occurrence of the spiral TG vortices as showed in figure 5. With increasing Taylor number, they remain approximately constant. But beyond around T_{C7}=680, they suddenly decrease, because the velocity fluctuations attenuate and become zero. We shall call this phenomenon as the relaminarization. Koichi Nakabayachi and coauthors [13,25] found numerically and experimentally by a laser Doppler velocimeter method the same behavior of the curve of our work.

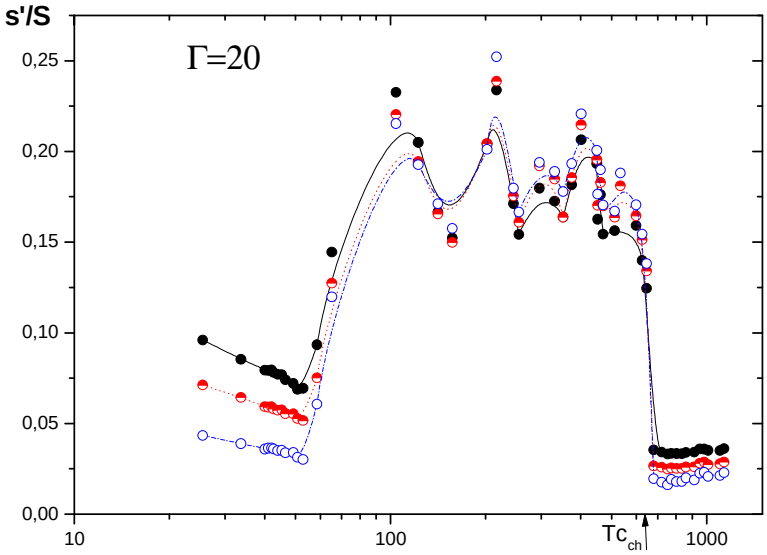

Figure 5: Evolution of non-dimensional fluctuations intensity, s'/S, versus Taylor number for Γ=20. Open circles for probe 1and solid circles for probe 2.

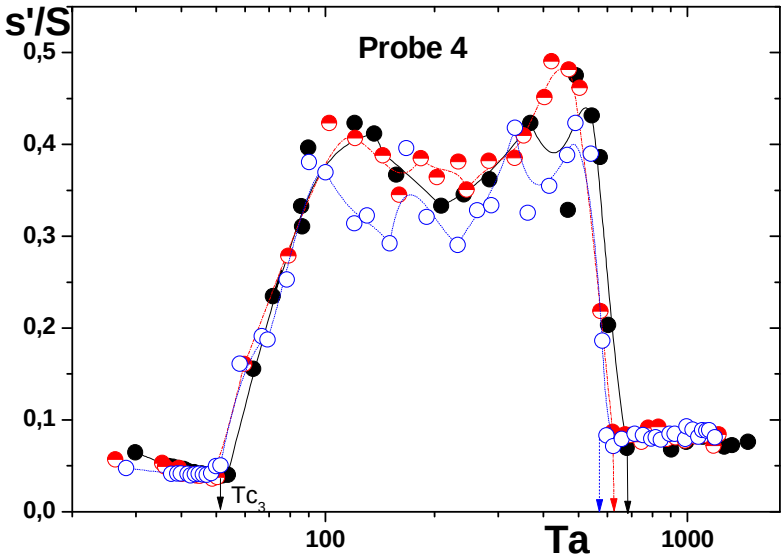

Figure 6: Evolution of non-dimensional fluctuations intensity, s'/S, versus Taylor number for different aspect ratio Γ. Solid circles stand for Γ=20, half solid circles for Γ=19 and open circles for Γ=18.

Wavy Taylor vortices and spirals, 53 ≤Ta <62

Regime composed of four wavy Taylor vortices at the equator and four spirals at each side of the Taylor cells occurred at a critical value Tc_3= 53 (Fig. 4b). The amplitude of the waves increased with the distance from equator where it was very small. The wall velocity gradient increased with Taylor number (Fig.3), and varied with of meridian position and time. The amplitude of fluctuations s'/S increased rapidly with Taylor number (Figs 5 and 6).

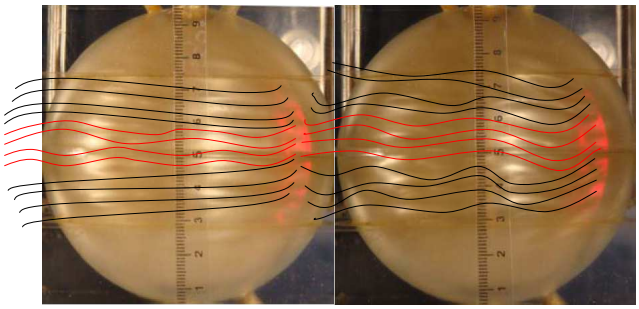

Figure 7: (a) Spiral Mode and Wavy Mode visualization, Ta=58. **(b)** Spiral Wavy Mode visualization, Ta=126.

Wavy Taylor vortices and wavy spirals, 62 ≤ Ta < 227

At the critical value Tc_4=62, four wavy Taylor vortices were present at the equator. The spirals in the rest of the gap became wavy (Fig. 7b).The spirals propagated slowly from the equator to the poles at an increasing velocity with time. The mean value of wall velocity gradient versus Ta increased in all measured positions (Fig. 3). The experimental absolute value uncertainty in wall shear rate measurements, was of 7%.

At a critical number Tc_5=227, azimuthal waves in the entire gap were observed (Fig. 9). With increasing speed, the flow pattern becomes progressively chaotic.

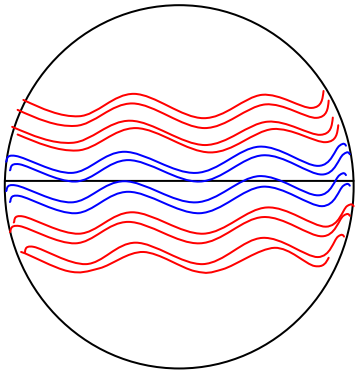

Figure 9: Wavy mode.

Turbulent regime, Ta ≥ 465

The near-turbulence regime manifested itself by the appearance of fluctuations at the poles at a Taylor number of Tc_6=465. These fluctuations propagated gradually into the equatorial part.

With an increase in rotation rate the azimuthal waves gradually attenuated. At a critical value of Tc_7=680 the flow in four Taylor vortices at the equator is turbulent and the rest of the gap is filled with chaotic flow (Fig. 10). The power spectrum was flat without any dominant frequency (Fig.8). The two electrodes showed a sharp drop of fluctuations at Ta=680 (Fig. 5) and this drop occurred also at different aspect ratios (Fig. 6).

At a critical value Tc_8=1192, a regime of fully developed turbulence started in the whole gap.

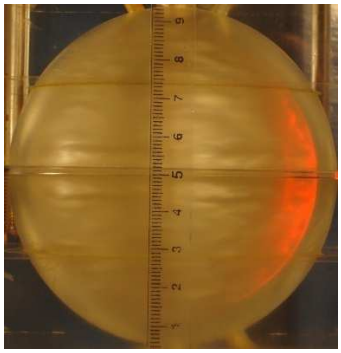

Figure 10: Chaotic flow at Ta=680.

4 Conclusions

The polarographic technique is used for the first time in the configuration of the device for measuring spherical parietal velocity gradient.
Thus, the critical values and the route to chaos are determined. Taylor vortices were observed at low Taylor numbers ($44 < Ta < 47$). They occurred gradually until the appearance of four cells. With an increase in rotation rate, we got the following sequence of regimes: Taylor vortices and spirals ($47 \leq Ta < 53$), wavy Taylor vortices and spirals ($53 \leq Ta < 62$), wavy Taylor vortices and wavy spirals ($62 \leq Ta < 227$), chaotic regime ($227 \leq Ta < 465$), turbulent regime ($Ta \geq 465$) and fully developed turbulence ($Ta=1192$).

The analysis of the results and in particular the evolution of parietal velocity gradient in the number of Taylor helped to highlight the different flow regimes when gradually increasing the speed of rotation of the sphere. The evolution at the mean wall velocity gradient with Ta was linear until Ta=47, then the increase was more important until Ta=227.

An important increase of the fluctuations of the wall velocity gradient measured close to the equator started at Ta=53. The important fluctuations lasted until Ta=465, where a sharp decrease as the consequence of turbulent flow without any cell is observed At these Ta, the azimuthal waves gradually attenuated, fluctuations of chaotic type settled down and the flow degenerated to a fully turbulent motion at last.

The wavy modes were characterized by sharp peaks on power spectra where as the chaotic and turbulent flow resembled white noise.

Our experimental results by polarographic method are in good agreement with the root-mean-square values found by Nakabayashi et al [25] in the presence of laser-Doppler velocimetry probe in measurements of the flow. The polarographic method has the advantage of access to measurements at the inner wall of the outer sphere. We can conclude that both techniques complement for better exploration of the flow between the two spheres.

References

[1] G. N. Khlebutin, Stability of fluid motion between a rotating and a stationary concentric sphere, *Journal of Fluid Dyn*, vol.3 (1968) pp. 31-32.

[2] O. Sawatzti, J. Zierep, Das Stromungsfeld um eine rotierende Kugel, *Journal of Acta. Mech*, vol. 9, (1970) pp.159

[3] B. R. Munson, M. Menguturk, Experimental results for low Reynolds number flow between eccentric rotating spheres, *Journal of Fluid Mech*, vol. 18, no. 2 (1975) pp.128-130.

[4] I. M. Yavorskaya, Yu. N. Belyaev, A. A. Monakhov, N. M. Astaf'eva, S. A. Scherbakov, N. D. Vvedenskaya, Stability, non-uniqueness and transition to turbulence in the flow between two rotating spheres, IUTAM-Symposium, Toronto, Canada, 1980.

[5] M. Wimmer, Experiments on the stability of viscous flow between two concentric rotating spheres, *Journal of Fluid Mech*, vol. 103 (1981) pp.117-131.

[6] M. Wimmer, Experiments on a viscous fluid between concentric rotating spheres, *Journal of Fluid Mech*, vol. 78 (1981) pp.317-335.

[7] K. Bühler, J. Zierep**,** (1984) New secondary instabilities for high Re-number flow between two rotating spheres, in: Kozolov, V.V. (ed.): Laminar-Turbulent Transition. IUTAM-Symp, Novosibirsk/USSR, *Springer*, vol. 1985, pp. 677-685.

[8] K. Bühler, Symmetric and asymmetric Taylor vortex flow in spherical gaps, *Journal of Acta Mech*, vol. 81 (1990) pp.3-38.

[9] G. Schrauf, The first instability in spherical Taylor–Couette flow, *Journal of Fluid Mech*, vol. 166 (1986) pp.287–303.

[10] C. Egbers, H. J. Rath, The existence of Taylor vortices and wide-gap instabilities in spherical Couette flow, *Journal of Acta Mech*, vol. 111 (1995) pp.125-140.

[11] R. Hollerbach, Time-dependent Taylor vortices in wide-gap spherical Couette flow, *Phys Rev Lett*, vol. 81 (1998) pp.3132-3135.

[12] M. Wimmer, Experiments on a viscous fluid flow between rotating spheres, *Journal of Fluid Mech*, vol. 79 (1976) pp.317-335.

[13] K. Nakabayashi, W. Sha, Vortical structures and velocity fluctuations of spiral and wavy vortices in the spherical Couette Flow, *Springer-Verlag Berlin Heidelberg LNP*, vol. 549 (2000) pp.234–255.

[14] D. Schmitt, T. A. Siere, D. Brito, P. Cardin, N. `Re. Gagnie, D. Jault, H. C. Nataf, Rotating spherical Couette flow in a dipolar magnetic field: experimental study of magneto-inertial waves, *Journal of Fluid Mech*, vol. 604 (2008) pp.175–197.

[15] P. Bar-Yoseph, A. Solan, R. Hillen, K. G. Roesner, Taylor vortex flow between eccentric coaxial rotating spheres, *Journal of Phys Fluids*, vol. 2 (1990) pp.1564-1573.

[16] P. Bar-Yoseph, K. G. Roesner, A. Solan, Vortex breakdown in the polar region between rotating spheres, *Journal of Phys. Fluids*, vol. 4 (1992) pp.1677-1686.

[17] C. K. Mamun, L. S. Tuckerman, Asymmetry and Hopf bifurcation in spherical Couette flow, *Journal of Phys Fluids*, vol. 7 (1995) pp.80-91.

[18] R. J. Yang, A numerical procedure for predicting multiple solutions of a spherical Taylor-Couette flow, Int J Numer Methods Fluids, vol. 22 (1996) pp.1135-1147.

[19] Li. Yuan, Numerical investigation of wavy and spiral Taylor-Gortler vortices in medium spherical gaps, *Journal of Physics of Fluids*, vol. 24 (2012) 124104.

[20] D. H. Kelly, S. A. Triana, D. S. Zimmerman, D. P. Lathrop, Selection of inertial modes in spherical Couette flow, *Journal of Phys Rev E*, vol. 81, 026311 (2010).

[21] G. Cognet, Utilisation de la polarographie pour l'étude de l'écoulement de Couette. *Journal of Mécanique*, vol. 10 (1971) pp.65-90.

[22] M. A. Leveque, Les lois de la transmission de chaleur par convection. *Ann Mines*, vol. 13 (1928) pp.201.

[23] F. Bartels, Taylor vortices between two concentric rotating spheres, *Journal of Fluid Mech*, vol. 119 (1982) pp.1-25.

[24] K. Nakabayashi, Transition of Taylor-Gortler vortex flow in spherical Couette flow, *Journal of Fluid Mech*, vol. 132 (1983) pp.209-230.

[25] K. Nakabayashi, W. Sha, Yoichi Tsuchida, Relaminarization phenomena and external-disturbance effects in spherical Couette Flow, *Journal of fluid mech* 534 (2005) pp.327–350.